

Design and analysis of vibration energy harvesters based on peak response statistics

S Adhikari¹, M I Friswell¹, G Litak^{2,3} and H Haddad Khodaparast¹

¹ College of Engineering, Swansea University, Bay Campus, Fabian Way, Crymlyn Burrows, Swansea, SA1 8EN, UK

² Lublin University of Technology, Faculty of Mechanical Engineering, Nadbystrzycka 36, 20-618 Lublin, Poland

E-mail: S.Adhikari@swansea.ac.uk, M.I.Friswell@swansea.ac.uk, g.litak@pollub.pl and H.HaddadKhodaparast@swansea.ac.uk

Received 19 November 2015, revised 18 February 2016

Accepted for publication 11 April 2016

Published 11 May 2016



CrossMark

Abstract

Energy harvesting using cantilever piezoelectric vibration energy harvesters excited by Gaussian broadband random base excitation is considered. The optimal design and analysis of energy harvesters under random excitation is normally performed using the mean and standard deviation of a response quantity of interest, such as the voltage. An alternative approach based on the statistics of the peak voltage is developed in this paper. Three extreme response characteristics, namely (a) level crossing, (b) response peaks above certain level, and (c) fractional time spend above a certain level, have been employed. Two cases, namely the harvesting circuit with and without an inductor, have been considered. Exact closed-form expressions have been derived for number of level crossings, statistics of response peaks and fractional time spend above a certain level for the output voltage. It is shown that these quantities can be related to the standard deviation of the voltage and its derivative with respect to time. Direct numerical simulation has been used to validate the analytical expressions. Based on the analytical results, closed-form expressions for optimal system parameters have been proposed. Numerical examples are given to illustrate the applicability of the analytical results.

Keywords: piezoelectric energy harvesting, random vibrations, broadband excitation, low voltage peaks

(Some figures may appear in colour only in the online journal)

1. Introduction

Scavenging of electrical energy from a vibrating piezoelectric device has received considerable attention in the last few years [1–3]. The use of these devices is crucial, particularly in applications where the deployment of batteries is often hampered by their limited lifespan, costly maintenance and complex recycling process. An example of the importance of these devices is in wildlife tracking technology in which replacing batteries is not only expensive and time consuming, also causes danger to the live-trapping of wild animals [4].

One of the main aspects in the design of an energy harvesting device is to ensure that it is tailored to the ambient energy available. There have been many potential applications for energy harvesting from broadband and random ambient excitation, for example aircraft noise. In this case, the harvester must be designed in a way that maximises the harvested energy from this form of excitation.

Harvesting energy from mechanical vibration sources can be achieved through piezoelectrics [5–7], ionic polymer metal composites [8, 9], magnetostrictive materials [10], and shape memory alloys [11]. Piezoelectric materials have been generally demonstrated to offer great potential due to their reliable and efficient performance as well as their compatibility

³ Author to whom any correspondence should be addressed.

with established fabrication processing at macro-, micro-, and even nano-scales [12]. There is currently a large number of applications for vibrating piezoelectric devices, ranging from wireless sensors for human and structural health monitoring to portable and small electronics [13–19]. The two most common types of piezoelectric materials are piezoceramics and piezopolymers [20]. The electromechanical coupling constant of piezoceramics is large and therefore is very useful in providing high energy conversion rate. However, they are too brittle and therefore cannot be used for energy harvesting in the mechanical devices with large elastic deformations, e.g. flexible beams. On the contrary, piezopolymers are much more flexible, which make them more useful in energy harvesting from flexible devices, albeit they suffer from a lower electromechanical coupling constant.

The design and subsequent application of piezoelectric energy harvesters depends on the nature of the excitation. Physically, the ambient excitations fall into two broad categories, namely narrow band excitations or broadband excitations. Mathematically, these two types of excitation are modelled by deterministic and random processes respectively. Energy harvesting systems with deterministic excitations have been the subject of extensive research over the past decade. We refer to the book by Erturk and Inman [21] for comprehensive details. Early works on vibration energy harvesting due to random excitations [22–25] considered Gaussian broadband excitation of linear and nonlinear harvesters. Subsequently several publications [26–47] proposed analytical, numerical and optimisation approaches for energy harvesters with random excitations. Most of these works consider ensemble average properties of the quantity of interests, such as the voltage or harvested power. Although the ensemble average gives an overall quantitative description of the response quantity, by its very nature, it may mask some details of the response which may be obtained in the time-domain. Considering the voltage, which is a random process [48] due to random excitations, some questions of potential interest are:

- How many times the output voltage of an energy harvester crosses a certain threshold within a given time interval?
- Can we quantitatively describe the nature of the peak of the voltage?
- For a given time interval, what is the percentage of time the output voltage would be above a certain level?

The answers to these questions could have a profound impact on the design of an energy harvester in the context of its intended application. For example, *a priori* knowledge of voltage peaks could safeguard associated electronic circuits. On the other hand, the knowledge of the percentage of time the output voltage remains above a certain level may lead to a superior utilisation of capacitors. If the answers to the above quantities are known, another intriguing possibility would be to optimise the system parameters so that the peak voltage satisfies certain design requirements. The incorporation of the consideration of ‘extreme values’ would result in an energy harvester which would be superior to what can be obtained by

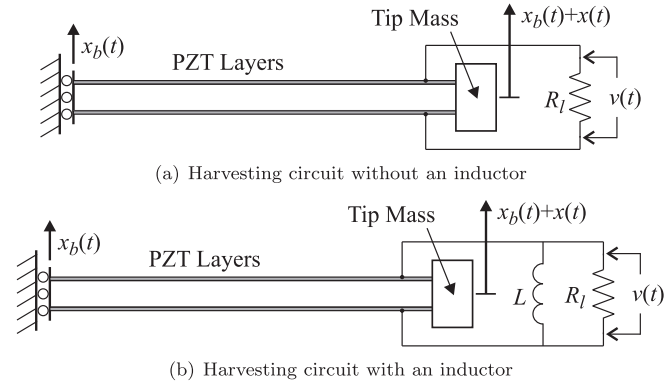


Figure 1. Schematic diagrams of piezoelectric energy harvesters with two different harvesting circuits.

simply considering average properties, as mostly adopted in the literature.

This paper develops new approaches for the design and analysis of vibration energy harvesters based on different extreme value characterisations of the voltage response. The excitation of the system is assumed to be broadband Gaussian white noise. In section 2, the single-degree-of-freedom electromechanical model is briefly reviewed and basic equations describing the system are described. The statistics of the peak response of the voltage random process is discussed in detail in section 3. The number of crossings of the voltage above a certain level is derived in section 3.1. In section 3.2 the statistics of the peaks of the voltage are discussed. The fractional occupation time of the voltage above a critical level is explained in section 3.3. Peak voltage statistics for systems without an inductor are derived in section 4, while the same statistics for systems with an inductor are derived in section 5. Closed-form expressions for the optimal parameters to maximise power for both cases are also derived. The analytical expressions derived in the paper are verified numerically in section 6.

2. Single degree of freedom electromechanical model

Various types of piezoelectric harvesting devices are available, integrating stack or patch transducers. Often these can be represented mechanically as a single degree of freedom system, particularly when the excitation is bandlimited and the natural frequencies are well separated. A typical example is the beam type harvester shown in figure 1, where the tip mass is used to increase the strain in the piezoelectric material and to increase the separation between the first and second natural frequencies. The two typical types of circuits, namely without and with an inductor, are shown in figures 1(a) and (b) respectively. A more detailed model of the cantilever beam harvester, along with correction factors for a single degree of freedom model that accounts for distributed mass effects, was given by Erturk and Inman [49–52]. This enables the analysis described here to be used in a wide range of practical applications, providing that the broadband base acceleration does not excite higher vibration modes of the harvester. The single degree of freedom

model could be extended to multi degree of freedom mechanical systems by using a modal decomposition of the response. This paper only considers a linear model of the piezoelectric material, which allows the application of linear random vibration theory. Many practical energy harvesting devices have nonlinearities not only in the mechanical vibration, but also the circuits are nonlinear in nature [53–56]. The relaxation of the linearity assumption would require the use of nonlinear random vibration theory which is not considered in this initial work. Under certain restrictive assumptions [30], the equivalent linearisation approach can be adopted to exploit some of the results derived in this paper.

2.1. Circuit without an inductor

The coupled electromechanical behaviour of the energy harvester can be expressed (see, for example [24, 57]) by linear ordinary differential equations as

$$m\ddot{x}(t) + c\dot{x}(t) + kx(t) - \theta v(t) = f_b(t), \quad (1)$$

$$C_p \dot{v}(t) + \frac{1}{R_l} v(t) + \theta \dot{x}(t) = 0. \quad (2)$$

Here, the force due to base excitation is given by

$$f_b(t) = -m\ddot{x}_b(t). \quad (3)$$

Equation (1) is simply Newton's equation of motion for a single degree of freedom system, where t is the time, $x(t)$ is the displacement of the mass, m , c and k are respectively the modal mass, modal damping and modal stiffness of the harvester and $x_b(t)$ is the random base excitation. In this paper we consider the base excitation to be a random process. The electrical load resistance is R_l , θ is the electromechanical coupling, and the mechanical force is modelled as proportional to the voltage across the piezoceramic, $v(t)$. Equation (2) is obtained from the electrical circuit, where the voltage across the load resistance arises from the mechanical strain through the electromechanical coupling, θ , and the capacitance of the piezoceramic, C_p . We refer to the book by Erturk and Inman [21] for further details on this model.

We assume that $f_b(t)$ is a weakly stationary Gaussian random process [48]. Therefore, its autocorrelation function depends only on the difference in the time instants, and thus

$$E[f_b(\tau_1)f_b(\tau_2)] = R_{f_b f_b}(\tau_1 - \tau_2). \quad (4)$$

This autocorrelation function can be expressed as the inverse Fourier transform of the spectral density $\Phi_{f_b f_b}(\omega)$ as

$$R_{f_b f_b}(\tau_1 - \tau_2) = \int_{-\infty}^{\infty} \Phi_{f_b f_b}(\omega) \exp[i\omega(\tau_1 - \tau_2)] d\omega. \quad (5)$$

A constant spectral density $\Phi_{f_b f_b}(\omega)$, which represents the case of white noise, is assumed in this paper. However, analytical results can be extended to the case when the base excitation is coloured Gaussian noise.

Transforming equations (1) and (2) into the frequency domain we obtain

$$\begin{bmatrix} -m\omega^2 + ci\omega + k & -\theta \\ i\omega\theta & i\omega C_p + \frac{1}{R_l} \end{bmatrix} \begin{Bmatrix} X(\omega) \\ V(\omega) \end{Bmatrix} = \begin{Bmatrix} F_b(\omega) \\ 0 \end{Bmatrix}. \quad (6)$$

Hence the frequency domain description of the displacement and the voltage can be obtained by inverting the coefficient matrix as

$$\begin{aligned} \begin{Bmatrix} X(\omega) \\ V(\omega) \end{Bmatrix} &= \frac{1}{\Delta_1(i\omega)} \begin{bmatrix} i\omega C_p + \frac{1}{R_l} & \theta \\ -i\omega\theta & -m\omega^2 + ci\omega + k \end{bmatrix} \begin{Bmatrix} F_b \\ 0 \end{Bmatrix} \\ &= \begin{Bmatrix} \left(i\omega C_p + \frac{1}{R_l}\right) F_b / \Delta_1 \\ -i\omega\theta F_b / \Delta_1 \end{Bmatrix}, \end{aligned} \quad (7)$$

where the determinant of the coefficient matrix is

$$\begin{aligned} \Delta_1(i\omega) &= mC_p(i\omega)^3 + (m/R_l + cC_p)(i\omega)^2 \\ &\quad + (kC_p + \theta^2 + c/R_l)(i\omega) + k/R_l. \end{aligned} \quad (8)$$

In the time domain, equations (1) and (2) can be expressed in the state-space form as

$$\frac{dz_1(t)}{dt} = \mathbf{A}_1 z_1(t) + \mathbf{B}_1 f_b(t). \quad (9)$$

Here the state-vector \mathbf{z} and corresponding coefficient matrices are defined as

$$\begin{aligned} \mathbf{z}_1(t) &= \begin{Bmatrix} x(t) \\ \dot{x}(t) \\ v(t) \end{Bmatrix}, \quad \mathbf{A}_1 = \begin{bmatrix} 0 & 1 & 0 \\ -k/m & -c/m & \theta/m \\ 0 & -\theta/C_p & -1/(C_p R_l) \end{bmatrix}, \\ \text{and } \mathbf{B}_1 &= \begin{bmatrix} 0 \\ 1/m \\ 0 \end{bmatrix}. \end{aligned} \quad (10)$$

Equation (9) can be solved with suitable initial conditions and elements of the state-vector can be obtained. The interest of this paper is to analyse the nature of the voltage $v(t)$ when the forcing function is a random process.

2.2. Circuit with an inductor

For this case the electrical equation (see for example, [58]) becomes

$$C_p \ddot{v}(t) + \frac{1}{R_l} \dot{v}(t) + \frac{1}{L} v(t) + \theta \dot{x}(t) = 0, \quad (11)$$

where L is the inductance of the circuit. The mechanical equation is the same as given in equation (1). Transforming equation (11) into the frequency domain one obtains

$$-\omega^2 \theta X(\omega) + \left(-\omega^2 C_p + i\omega \frac{1}{R_l} + \frac{1}{L} \right) V(\omega) = 0. \quad (12)$$

Similar to equation (6), this equation can be written in matrix form with the equation of motion of the mechanical system as

$$\begin{aligned} \begin{bmatrix} -m\omega^2 + ci\omega + k & -\theta \\ -\omega^2 \theta & -\omega^2 C_p + i\omega \frac{1}{R_l} + \frac{1}{L} \end{bmatrix} \\ \times \begin{Bmatrix} X(\omega) \\ V(\omega) \end{Bmatrix} &= \begin{Bmatrix} F_b(\omega) \\ 0 \end{Bmatrix}. \end{aligned} \quad (13)$$

Inverting the coefficient matrix, the displacement and voltage in the frequency domain can be obtained as

$$\begin{cases} X(\omega) \\ V(\omega) \end{cases} = \frac{1}{\Delta_2} \begin{bmatrix} -\omega^2 C_p + i\omega \frac{1}{R_l} + \frac{1}{L} & \theta \\ \omega^2 \theta & -m\omega + ci\omega + k \end{bmatrix} \\ \times \begin{cases} F_b \\ 0 \end{cases} = \begin{cases} \left(-\omega^2 C_p + i\omega \frac{1}{R_l} + \frac{1}{L} \right) F_b / \Delta_2 \\ \omega^2 \theta F_b / \Delta_2 \end{cases}. \quad (14)$$

Here the determinant of the coefficient matrix is a fourth-order polynomial in $(i\omega)$ and is given by

$$\begin{aligned} \Delta_2(i\omega) = & mC_p(i\omega)^4 + \frac{(cC_p R_l L + mL)}{R_l L} (i\omega)^3 \\ & + \frac{(mR_l + cL + \theta^2 R_l L + kC_p R_l L)}{R_l L} (i\omega)^2 \\ & + \frac{(cR_l + kL)}{R_l L} (i\omega) + \frac{k}{L}. \end{aligned} \quad (15)$$

In the time domain, equations (1) and (11) can be expressed in the state-space form as

$$\frac{d\mathbf{z}_2(t)}{dt} = \mathbf{A}_2 \mathbf{z}_2(t) + \mathbf{B}_2 f_b(t). \quad (16)$$

Here the state-vector \mathbf{z} and corresponding coefficient matrices are defined as

$$\mathbf{z}_2(t) = \begin{Bmatrix} x(t) \\ \dot{x}(t) \\ v(t) \\ \dot{v}(t) \end{Bmatrix}, \\ \mathbf{A}_2 = \begin{bmatrix} 0 & 1 & 0 & 0 \\ -k/m & -c/m & \theta/m & 0 \\ 0 & 0 & 0 & 1 \\ \theta k/mC_p & \theta c/mC_p & \theta^2/mC_p - 1/LC_p & -1/RC_p \end{bmatrix} \\ \text{and } \mathbf{B}_2 = \begin{bmatrix} 0 \\ 1/m \\ 0 \\ -\theta/mC_p \end{bmatrix}. \quad (17)$$

Equation (16) can be solved in a similar way as equation (9). As before, we are interested to analyse the nature of the voltage $v(t)$ when the forcing function is a random process.

3. Statistics of peak response of the voltage

We consider that the excitation force $f_b(t)$ is a random process. It is assumed that $f_b(t)$ is a weakly stationary, Gaussian, broadband random process so that its autocorrelation function is

$$R_{f_b f_b}(\tau_1 - \tau_2) = S_0 \delta(\tau_1 - \tau_2). \quad (18)$$

Here $\delta(\bullet)$ is the Dirac delta function and S_0 is the strength of the random process. Since the forcing $f_b(t)$ is assumed to be a delta-correlated random process, according to equation (3) the

base excitation, $x_b(t)$, is not a delta-correlated random process. However, due to the linear relationship in equation (3), the power-spectral density of the two processes can be related easily. Mechanical systems driven by this type of excitation have been discussed by Lin [59], Nigam [60], Bolotin [61], Roberts and Spanos [62] and Newland [63] within the scope of random vibration theory. To obtain the samples of the random response quantities such as the displacement of the mass $x(t)$ and the voltage $v(t)$, one needs to solve the coupled stochastic differential equations (1) and (2) or (1) and (11).

It is known that a linear dynamic system excited by a stationary, Gaussian random process will also result in a stationary, Gaussian random process with different spectral characteristics. Analytical results developed within the theory of random vibration allows us to obtain key properties of the peak values of the response process in closed-form. We are interested in the harvested power given by

$$P(t) = \frac{v^2(t)}{R_l}. \quad (19)$$

Although $v(t)$ is a stationary, Gaussian random process, $P(t)$ is in general a non-Gaussian random process due to the square operation as above. To understand the efficiency and long-term reliability of an energy harvester, it is necessary to quantify when the harvester power is above a certain critical level, say P_c . Mathematically, we want to obtain the statistical description of

$$P(t) \geq P_c. \quad (20)$$

In general, non-Gaussian processes such as $P(t)$ are difficult to deal with analytically. Therefore, this condition is expressed in terms of the voltage as

$$v(t) \geq v_c \quad \text{or} \quad v(t) \leq -v_c \quad \text{where} \quad v_c = \sqrt{P_c R_l}. \quad (21)$$

Since, in general, we consider random processes with zero mean, it is sufficient to investigate either of the above two conditions as statistically the peaks are symmetrically distributed about 0. Following Nigam [60], in the next subsections we discuss three main properties of the random process $v(t)$ related to the case $v(t) \geq v_c$.

3.1. Level crossing of the voltage

The voltage random process $v(t)$ is the third element of the random vector $\mathbf{z}(t)$ in equation (9). Since $f_b(t)$ is a stationary, Gaussian random process and the system under consideration is linear in nature, $v(t)$ is also a stationary, Gaussian random process. Additionally, $v(t)$, $t \in [0, T]$ for some T is a continuous and differentiable function. A representative sample of the random process $v(t)$ is shown in figure 2. The up-crossing of level v_c (with positive slope) and down-crossing of level v_c (with negative slope) are marked in the figure 3. Peaks appearing above the level v_c are also illustrated in figure 2.

The number of crossings of the level $v(t) = v_c$ within a time interval T is a discrete random variable. We define a

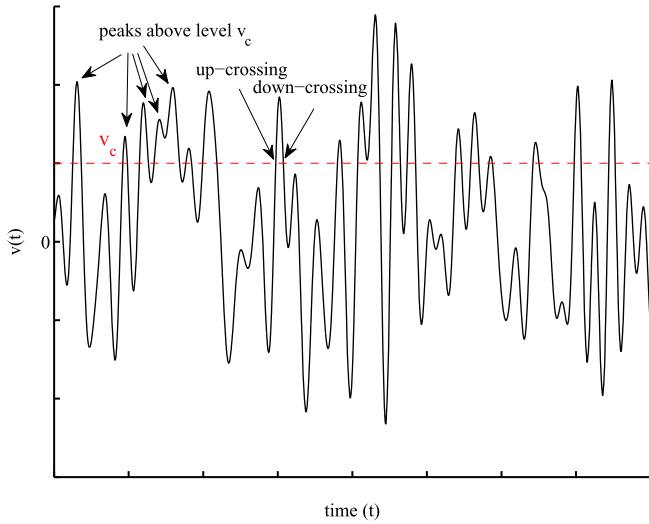


Figure 2. An example of up-crossings, down-crossings and peaks of the random voltage process $v(t)$ above a level $v(t) = v_c$.

zero-one counting process $Y_c(t)$ as

$$Y_c(t) = \begin{cases} 0 & \text{if } v(t) < v_c \\ 1 & \text{if } v(t) \geq v_c. \end{cases} \quad (22)$$

This can be defined in terms of unit step function $U(\bullet)$ as

$$Y_c(t) = U(v(t) - v_c). \quad (23)$$

The random process $Y_c(t)$ is effectively a counting functional which takes the values of 1 and 0 whenever the voltage $v(t)$ is above or below the level v_c . The slope of $v(t)$ can be included by differentiating $Y_c(t)$ with respect to time t as

$$\dot{Y}_c(t) = \dot{v}(t)\delta(v(t) - v_c) = \mathcal{N}(v_c, t), \quad (24)$$

where $\delta(\bullet)$ is the Dirac delta function. The random process $\dot{Y}_c(t)$ is a crossing rate functional, that is, $\mathcal{N}(v_c, t)$ representing an impulse every-time a crossing of level v_c occurs. The sign of the impulse clearly depends on the sign of $\dot{v}(t)$. Suppose $\mathcal{N}(v_c, T)$ is a counting process giving the *total* number of impulses in an interval $(t_0, t_0 + T]$ corresponding to both up and down crossings. Then

$$\begin{aligned} \mathcal{N}(v_c; T) &= \int_{t_0}^{t_0+T} \mathcal{N}(v_c, t) dt \\ &= \int_{t_0}^{t_0+T} |\dot{v}(t)|\delta(v(t) - v_c) dt. \end{aligned} \quad (25)$$

The average value of the number of crossings is then obtained by taking the mathematical expectation as

$$\begin{aligned} N(v_c; T) &= E[\mathcal{N}(v_c; T)] \\ &= \int_{t_0}^{t_0+T} E[|\dot{v}(t)|\delta(v(t) - v_c)] dt. \end{aligned} \quad (26)$$

Suppose $p(v, \dot{v}, t)$ denotes the joint probability density function (pdf) of $v(t)$ and $\dot{v}(t)$. Using this, together with the definition of the expectation operator, the above integral can

be evaluated as

$$\begin{aligned} N(v_c; T) &= \int_{t_0}^{t_0+T} \int_{-\infty}^{\infty} \int_{-\infty}^{\infty} |\dot{v}(t)|\delta \\ &\quad \times (v(t) - v_c)p(v, \dot{v}, t) dv d\dot{v} dt \\ &= \int_{t_0}^{t_0+T} \int_{-\infty}^{\infty} |\dot{v}(t)|p(v_c, \dot{v}, t) d\dot{v} dt \\ &= \int_{t_0}^{t_0+T} N(v_c; t) dt, \end{aligned} \quad (27)$$

where $N(v_c; t)$ represents the total *expected* rate of crossings of level v_c

$$N(v_c; t) = \int_{-\infty}^{\infty} |\dot{v}(t)|p(v_c, \dot{v}, t) d\dot{v} = N^+(v_c; t) + N^-(v_c; t). \quad (28)$$

Here $N^+(v_c; t)$ and $N^-(v_c; t)$ represent expected up and down crossing rate respectively and can be expressed by splitting the above integral as

$$\begin{aligned} N^+(v_c; t) &= \int_0^{\infty} \dot{v}(t)p(v_c, \dot{v}, t) d\dot{v} \\ \text{and } N^-(v_c; t) &= - \int_{-\infty}^0 \dot{v}(t)p(v_c, \dot{v}, t) d\dot{v}. \end{aligned} \quad (29)$$

The mathematical derivation so far is general in nature and does not depend on the assumptions of stationarity and Gaussianity of the random process $v(t)$. Below we make use of the simplification that the voltage $v(t)$ is a stationary Gaussian random process. It is well known [59, 60] that a stationary Gaussian random process and its derivative process are statistically independent. That is

$$E[v(t)\dot{v}(t)] = 0. \quad (30)$$

This allows the joint pdf $p(v, \dot{v}, t)$ to be expressed as the product of two separate pdfs as $p(v, \dot{v}, t) = p(v, t)p(\dot{v}, t)$. Assuming that the standard deviations of $v(t)$ and $\dot{v}(t)$ are σ_v and $\sigma_{\dot{v}}$ respectively, the joint pdf can be expressed as

$$\begin{aligned} p(v, \dot{v}) &= \frac{1}{\sqrt{2\pi}\sigma_v} \exp\left(-\frac{v^2}{2\sigma_v^2}\right) \times \frac{1}{\sqrt{2\pi}\sigma_{\dot{v}}} \exp\left(-\frac{\dot{v}^2}{2\sigma_{\dot{v}}^2}\right) \\ &= \frac{1}{2\pi\sigma_v\sigma_{\dot{v}}} \exp\left\{-\left(\frac{v^2}{2\sigma_v^2} + \frac{\dot{v}^2}{2\sigma_{\dot{v}}^2}\right)\right\}. \end{aligned} \quad (31)$$

Substituting this joint pdf into equation (29), the integrals can be evaluated in closed-form as

$$\begin{aligned} N^+(v_c) &= N^-(v_c) = p(v_c) \int_0^{\infty} \dot{v}p(\dot{v}) d\dot{v} \\ &= \frac{1}{2\pi} \frac{\sigma_{\dot{v}}}{\sigma_v} \exp\left(-\frac{v_c^2}{2\sigma_v^2}\right). \end{aligned} \quad (32)$$

This gives an explicit expression of the expected rate of crossing the level $v(t) = v_c$. The rate of crossing zero can be obtained by substituting $v_c = 0$ in the above expression to

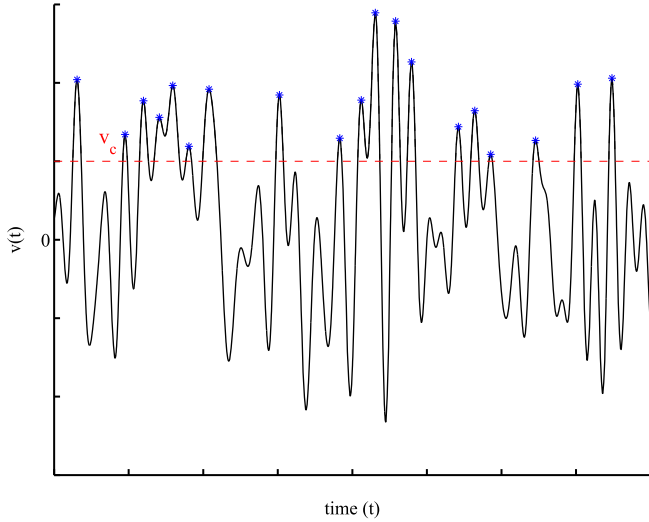


Figure 3. Peaks of the voltage $v(t)$ above the level v_c (denoted by *).

give

$$N^+(0) = N^-(0) = \frac{1}{2\pi} \frac{\sigma_{\dot{v}}}{\sigma_v}. \quad (33)$$

The crossing rate of the voltage only depends on the standard deviation of voltage and its derivative. In section 3.4, the calculation of these quantities will be discussed.

3.2. Statistics of voltage peaks

The excitation $f_b(t)$ is assumed to be broadband excitation as it represents the most realistic ambient excitation. In contrast, the response quantities $x(t)$ and $v(t)$, and their derivatives are, in general, expected to be narrowband random processes with peaks around the deterministic resonance frequency of the system. For a narrowband stationary Gaussian random process, the expected number of peaks per unit time above the level $v(t) = v_c$ is equal to $N^+(v_c)$. A representative sample of the random process $v(t)$ and its peaks above the level v_c is shown in figure 3. The total number of peaks per unit time is $N^+(0)$. Therefore, using the relative frequency definition of probability we have

$$E\left[\frac{N^+(v_c)}{N^+(0)}\right] = \frac{E[N^+(v_c)]}{E[N^+(0)]} = \frac{N^+(v_c)}{N^+(0)}. \quad (34)$$

Thus, from the definition of probability, it follows that

$$\begin{aligned} P \text{ [occurrence of peaks above } v(t) = v_c] \\ = 1 - F_P(v_c) = \frac{N^+(v_c)}{N^+(0)}, \end{aligned} \quad (35)$$

where $F_P(v_c)$ is the pdf of the peaks above $v(t) = v_c$. Hence, using equations (32) and (33), we obtain

$$F_P(v_c) = 1 - \frac{N^+(v_c)}{N^+(0)} = 1 - \exp\left(-\frac{v_c^2}{2\sigma_v^2}\right). \quad (36)$$

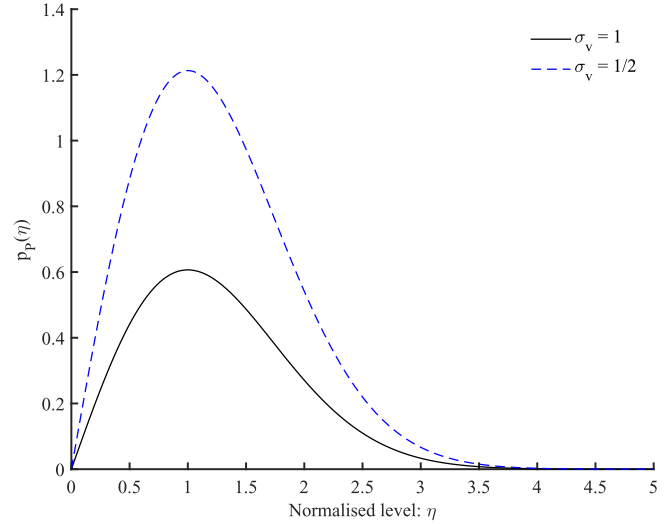


Figure 4. Probability density function of the peaks of the voltage $v(t)$ above the normalised level η for two representative values of the standard deviation of $v(t)$.

Differentiating with respect to v_c , we obtain the pdf of the occurrence of the peaks as

$$p_P(v_c) = \frac{dF_P(v_c)}{dv_c} = \frac{v_c}{\sigma_v^2} \exp\left(-\frac{v_c^2}{2\sigma_v^2}\right). \quad (37)$$

This implies that the distribution of peaks of the voltage follows a Rayleigh distribution [64]. Expressing the level v_c normalised with respect to the standard deviation as

$$v_c = \eta\sigma_v \quad (38)$$

we have

$$p_P(\eta) = \frac{\eta}{\sigma_v} \exp\left(-\frac{\eta^2}{2}\right). \quad (39)$$

In figure 4, this pdf is shown for two representative values of the standard deviation of $v(t)$, namely $\sigma_v = 1$ and $\sigma_v = 1/2$. This result shows that the probability of very large and very small peaks in the voltage is small compared to ‘average’ peaks.

3.3. Fractional occupation time of the voltage above a critical level

The fractional occupation time is defined as the proportion of time spent by the random process $v(t)$ above a desired level v_c . The quantification of fractional occupation time would be useful to predict harvested power from energy harvesting devices operating for long periods of time. It may be possible to optimise system parameters so that the fractional occupation time is maximised. A representative sample of the random process $v(t)$ and the intervals of time spend above the level v_c is shown in figure 5. The fractional occupation time within an interval T is a random variable $Z_{v_c}(T)$ whose value lies between 0 and 1. This can be expressed in terms of the

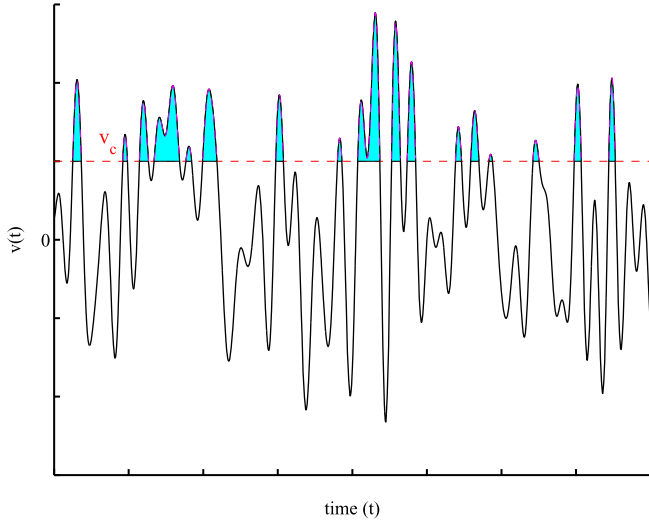


Figure 5. Fraction of time spent by voltage $v(t)$ above the level v_c (the shaded area).

zero-one process $Y_c(t)$ defined in equation (23) as

$$Z_{v_c}(T) = \frac{1}{T} \int_{t_0}^{t_0+T} Y_c(t) dt. \quad (40)$$

Here we are interested in the mean of this random variable, that is $E[Z_{v_c}(T)]$. Using the definition of the expectation operator we have

$$\begin{aligned} E[Z_{v_c}(T)] &= \frac{1}{T} \int_{t_0}^{t_0+T} E[Y_c(t)] dt \\ &= \frac{1}{T} \int_{t_0}^{t_0+T} \int_{-\infty}^{\infty} U(v(t) - v_c) p(v, t) dv dt \\ &= \frac{1}{T} \int_{t_0}^{t_0+T} \int_{v_c}^{\infty} p(v, t) dv dt. \end{aligned} \quad (41)$$

Since $v(t)$ is a stationary Gaussian random process, the above integral can be evaluated as

$$\begin{aligned} E[Z_{v_c}(T)] &= \int_{v_c}^{\infty} p(v, t) dv = \int_{v_c}^{\infty} \frac{1}{\sqrt{2\pi}\sigma_v} \exp\left(-\frac{v^2}{2\sigma_v^2}\right) dv \\ &= \frac{1}{2} \operatorname{erfc}\left(\frac{v_c}{\sqrt{2}\sigma_v}\right), \end{aligned} \quad (42)$$

where $\operatorname{erfc}(\bullet)$ is the complimentary error function [65]. Equation (42) explicitly gives an expression of the average fractional occupation time of the voltage $v(t)$ above the level v_c . Using the normalised level in equation (38), the fractional occupational time can be obtained as

$$E[Z_\eta] = \frac{1}{2} \operatorname{erfc}\left(\frac{\eta}{\sqrt{2}}\right). \quad (43)$$

In figure 6, the fractional occupational time of the voltage $v(t)$ above the normalised level η is shown. When $\eta = 0$, the random process $v(t)$ spends half of the time above the zero level. The fractional occupational time reduces for increasing values of η as expected.

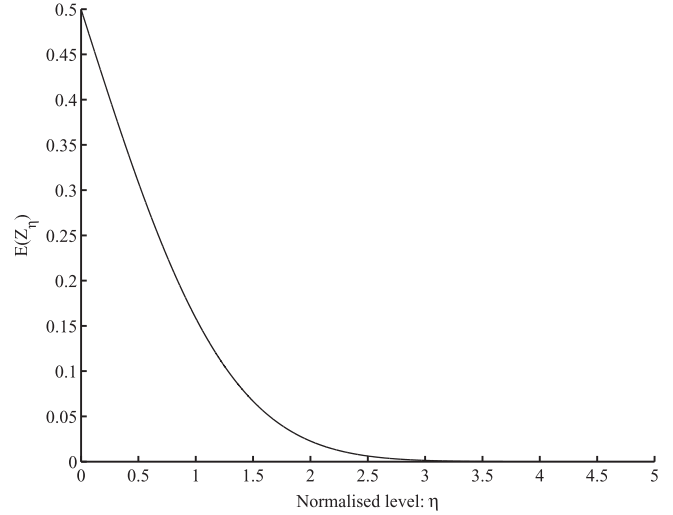


Figure 6. Fractional occupational time above the normalised level η of the voltage $v(t)$.

3.4. Calculation of standard deviations of voltage and its derivative

From the preceding sections it is clear that the standard deviation of the voltage and its derivative is necessary to obtain the crossing rate, peak statistics and the fractional occupational time. The analytical expressions given for these quantities are independent from the nature of the system (e.g., linearity). The system-specific aspect enters in this formulation through the standard deviation of the voltage and its derivative only. For a general nonlinear system, these functions can be obtained numerically. However, since a linear model is used in this study, we outline an approach to analytically obtain these quantities using the theory of random vibration. We adopt the technique developed by Roberts and Spanos [62], which was applied to the energy harvesting problem in [24].

As seen in section 2, for a linear energy harvesting system, the voltage in the frequency domain can be expressed in the form

$$V(\omega) = H(\omega)F_b(\omega). \quad (44)$$

It can be shown that [59, 60] the spectral density of V is related to the spectral density of F_b by

$$\Phi_{VV}(\omega) = H(\omega)H^*(\omega)\Phi_{f_b f_b}(\omega) = |H(\omega)|^2 \Phi_{f_b f_b}(\omega). \quad (45)$$

where $(\bullet)^*$ denote complex conjugation. Recall that the random process $v(t)$ has zero mean. Therefore, in the steady-state (large t), we obtain

$$\sigma_v^2 = E[v^2(t)] = R_{vv}(0) = \int_{-\infty}^{\infty} |H(\omega)|^2 \Phi_{f_b f_b}(\omega) d\omega. \quad (46)$$

In the frequency domain, the derivative process can be expressed as

$$\dot{V}(\omega) = (i\omega)V(\omega) = (i\omega)H(\omega)F_b(\omega). \quad (47)$$

Since $\dot{v}(t)$ is also a zero-mean stationary Gaussian random process, its standard deviation can be obtained in a similar

manner as

$$\sigma_v^2 = E[\dot{v}^2(t)] = \int_{-\infty}^{\infty} \{(i\omega)H(\omega)\} \{(i\omega)H(\omega)\}^* \times \Phi_{f_b f_b}(\omega) d\omega = \int_{-\infty}^{\infty} \omega^2 |H(\omega)|^2 \Phi_{f_b f_b}(\omega) d\omega. \quad (48)$$

The expressions of σ_v and $\sigma_{\dot{v}}$ are then substituted into the expressions derived in the previous three subsections.

The calculation of the integral on the right-hand side of equations (46) and (48) in general requires the calculation of integrals involving the ratio of polynomials of the following form

$$I_n = \int_{-\infty}^{\infty} \frac{\Xi_n(\omega) d\omega}{\Lambda_n(i\omega)\Lambda_n^*(i\omega)}. \quad (49)$$

Here the polynomials are expressed as

$$\Xi_n(\omega) = b_{n-1}\omega^{2n-2} + b_{n-2}\omega^{2n-4} + \dots + b_0, \quad (50)$$

$$\Lambda_n(i\omega) = a_n(i\omega)^n + a_{n-1}(i\omega)^{n-1} + \dots + a_0. \quad (51)$$

Following Roberts and Spanos [62] this integral can be evaluated as

$$I_n = \frac{\pi \det[\mathbf{N}_n]}{a_n \det[\mathbf{D}_n]}. \quad (52)$$

Here the $n \times n$ matrices are defined as

$$\mathbf{N}_n = \begin{bmatrix} b_{n-1} & b_{n-2} & \dots & b_0 \\ -a_n & a_{n-2} & -a_{n-4} & a_{n-6} & \dots & 0 & \dots \\ 0 & -a_{n-1} & a_{n-3} & -a_{n-5} & \dots & 0 & \dots \\ 0 & a_n & -a_{n-2} & a_{n-4} & \dots & 0 & \dots \\ 0 & \dots & \dots & \dots & \dots & 0 & \dots \\ 0 & 0 & \dots & \dots & \dots & -a_2 & a_0 \end{bmatrix} \quad (53)$$

and

$$\mathbf{D}_n = \begin{bmatrix} a_{n-1} & -a_{n-3} & a_{n-5} & -a_{n-7} & \dots & 0 & \dots \\ -a_n & a_{n-2} & -a_{n-4} & a_{n-6} & \dots & 0 & \dots \\ 0 & -a_{n-1} & a_{n-3} & -a_{n-5} & \dots & 0 & \dots \\ 0 & a_n & -a_{n-2} & a_{n-4} & \dots & 0 & \dots \\ 0 & \dots & \dots & \dots & \dots & 0 & \dots \\ 0 & 0 & \dots & \dots & \dots & -a_2 & a_0 \end{bmatrix}. \quad (54)$$

These expressions will be used for the two cases considered. We assume that the excitation $f_b(t)$ is Gaussian white noise so that its spectral density is constant with respect to frequency. But different spectral densities can be easily used within the scope of this formulation.

4. Peak statistics for systems without an inductor

4.1. Derivation of the standard deviations of voltage and its derivative

From equation (7) we obtain the voltage in the frequency domain as

$$V(\omega) = H(\omega)F_b \quad \text{where} \quad H(\omega) = -\frac{i\omega\theta}{\Delta_1(i\omega)}. \quad (55)$$

Since the forcing function has constant spectral density we assume that

$$\Phi_{f_b f_b}(\omega) = S_0. \quad (56)$$

Therefore, the standard deviation of $v(t)$ can be obtained using equation (46) as

$$\sigma_v^2 = \int_{-\infty}^{\infty} |H(\omega)|^2 S_0 d\omega = S_0 \theta^2 \int_{-\infty}^{\infty} \frac{\omega^2}{\Delta_1(i\omega)\Delta_1^*(i\omega)} d\omega. \quad (57)$$

From equation (8) one can observe that $\Delta_1(i\omega)$ is a third order polynomial in $(i\omega)$. Comparing the integral in equation (57) with the general integral in equation (49) we have

$$n = 3, b_2 = 0, b_1 = 1, b_0 = 0 \quad \text{and} \quad a_3 = mC_p, a_2 = (m/R_l + cC_p), \\ a_1 = (kC_p + \theta^2 + c/R_l), a_0 = k/R_l. \quad (58)$$

Now using equation (52), the integral can be evaluated as

$$\int_{-\infty}^{\infty} \frac{\omega^2}{\Delta_1(i\omega)\Delta_1^*(i\omega)} d\omega = \frac{\pi \det \begin{bmatrix} b_2 & b_1 & b_0 \\ -a_3 & a_1 & 0 \\ 0 & -a_2 & a_0 \end{bmatrix}}{a_3 \det \begin{bmatrix} a_2 & -a_0 & 0 \\ -a_3 & a_1 & 0 \\ 0 & -a_2 & a_0 \end{bmatrix}} = \frac{\pi \det \begin{bmatrix} 0 & 1 & 0 \\ -mC_p & kC_p + \theta^2 + c/R_l & 0 \\ 0 & -m/R_l - cC_p & k/R_l \end{bmatrix}}{mC_p \det \begin{bmatrix} m/R_l + cC_p & -k/R_l & 0 \\ -mC_p & kC_p + \theta^2 + c/R_l & 0 \\ 0 & -m/R_l - cC_p & k/R_l \end{bmatrix}}. \quad (59)$$

From equation (57) we then obtain the standard deviation of the voltage due to white-noise forcing as

$$\sigma_v^2 = \frac{S_0 \theta^2 \pi R_l^2}{cC_p^2 R_l^2 k + (cR_l^2 \theta^2 + c^2 R_l) C_p + m\theta^2 R_l + mc}. \quad (60)$$

The standard deviation of the derivative of the voltage $\dot{v}(t)$ can be obtained using equation (48) as

$$\sigma_{\dot{v}}^2 = \int_{-\infty}^{\infty} \omega^2 |H(\omega)|^2 \Phi_{f_b f_b}(\omega) d\omega = S_0 \theta^2 \int_{-\infty}^{\infty} \frac{\omega^4}{\Delta_1(i\omega)\Delta_1^*(i\omega)} d\omega. \quad (61)$$

This can be evaluated as for the previous case with

$$n = 3, b_2 = 1, b_1 = 0, b_0 = 0 \quad (62)$$

with the same a_i , for $i = 0, \dots, 3$. Forming the \mathbf{N}_3 and \mathbf{D}_3 matrices, and taking the ratio of the determinants of these

matrices, following equation (52), we have

$$\sigma_v^2 = \frac{S_0 \theta^2 \pi (k C_p R_l + \theta^2 R_l + c) R_l}{(c C_p^2 R_l^2 k + (c R_l^2 \theta^2 + c^2 R_l) C_p + m \theta^2 R_l + mc) m C_p}. \quad (63)$$

4.2. Parameter optimisation

The aim of this section is to investigate if there are any sets of parameters which maximises (a) the crossing rate of the voltage above the level v_c and, (b) the fractional occupational time above the level v_c . For a given vibration energy harvester, the mass and stiffness are usually selected from general consideration. Additionally, damping is generally kept as small as possible to maximise sustained vibration. Therefore, m , c , k are not considered as design parameters from the point of view of random excitation. The aim is to find optimal parameter values, or parametric relationships, for the resistance (R_l), electromechanical coupling (θ), and capacitance (C_p).

Using the expressions of σ_v and $\sigma_{\dot{v}}$ from equations (60) and (63), the zero crossing rate given by (33) can be calculated as

$$N^+(0) = N^-(0) = \frac{1}{2\pi} \frac{\sigma_{\dot{v}}}{\sigma_v} = \frac{1}{2\pi} \sqrt{\frac{k C_p R_l + \theta^2 R_l + c}{m C_p R_l}}. \quad (64)$$

Thus, the rate of zero crossing of the voltage can be obtained directly from the harvester parameters. Parameter values can also be selected to set a desired zero crossing rate.

Using the expressions of σ_v in equation (60), together with the expression of v_c in terms of desired power P_c in equation (21), the expected rate of crossing can be obtained from equation (32) as

$$N^+(P_c) = N^-(P_c) = \frac{1}{2\pi} \sqrt{\frac{k C_p R_l + \theta^2 R_l + c}{m C_p R_l}} \exp \left\{ - \frac{P_c (c C_p^2 R_l^2 k + (c R_l^2 \theta^2 + c^2 R_l) C_p + m \theta^2 R_l + mc)}{2 R_l \theta^2 \pi S_0} \right\}. \quad (65)$$

This gives an explicit formula of the expected rate of crossing the level of harvested power P_c . We aim to find parameter relationship such that this rate of crossing of power level P_c is maximised. Differentiating equation (65) with respect to the resistance R_l , setting the result to zero, and after some algebra, gives the necessary condition as

$$\begin{aligned} & (-2 C_p^2 P_c k \theta^2 - C_p P_c \theta^4 - C_p^3 P_c k^2) R_l^3 \\ & + (-C_p P_c \theta^2 c - C_p^2 P_c k c) R_l^2 \\ & + (-\pi \theta^2 S + m P_c k C_p + m P_c \theta^2) R_l + m P_c c = 0. \quad (66) \end{aligned}$$

This cubic equation can be solved to obtain an optimal value of R_l . Since such analytical expressions are complex in nature, we make use of a simplification that the damping of the system is negligible. Therefore, substituting $c = 0$, we

obtain an optimal value of the resistance as

$$R_{l_{opt}} = \frac{\sqrt{P_c C_p (m P_c (\theta^2 + k C_p) - \pi \theta^2 S_0)}}{P_c C_p (\theta^2 + k C_p)}. \quad (67)$$

Next we aim to maximise the average fractional occupation time of the voltage $v(t)$ above the level v_c given in equation (42). As seen in figure 6, the complimentary error function is a monotonically decreasing function of its argument. Therefore, it is necessary to minimise the argument $\frac{v_c}{\sqrt{2} \sigma_v}$. The square of this expression can be obtained in terms of the power level P_c as

$$\frac{P_c (c C_p^2 R_l^2 k + (c R_l^2 \theta^2 + c^2 R_l) C_p + m \theta^2 R_l + mc)}{2 R_l \theta^2 \pi S}. \quad (68)$$

Differentiating this with respect to R_l we obtain the necessary condition as

$$R_{l_{opt}} = \sqrt{\frac{m}{C_p (\theta^2 + k C_p)}}. \quad (69)$$

This expression matches exactly with the results obtained in [24] for maximum power.

5. Peak statistics for systems with an inductor

5.1. Derivation of the standard deviations of voltage and its derivative

From equation (14) we obtain the voltage in the frequency domain as

$$V(\omega) = H(\omega) F_b \quad \text{where} \quad H(\omega) = \omega^2 \theta / \Delta_2(i\omega). \quad (70)$$

Recalling that the forcing function has a constant spectral density S_0 , the standard deviation of $v(t)$ can be obtained using equation (46) as

$$\sigma_v^2 = \int_{-\infty}^{\infty} |H(\omega)|^2 S_0 d\omega = S_0 \theta^2 \int_{-\infty}^{\infty} \frac{\omega^4}{\Delta_2(i\omega) \Delta_2^*(i\omega)} d\omega. \quad (71)$$

From equation (15) one can observe that $\Delta_2(i\omega)$ is fourth-order polynomial in $(i\omega)$. Comparing the integral in equation (71) with the general integral in equation (49) we have

$$\begin{aligned} & n = 4, b_3 = 0, b_2 = 1, b_1 = 0, b_0 = 0 \\ \text{and} \quad & a_0 = \frac{k}{L}, a_1 = \frac{(c R_l + k L)}{R_l L}, \\ & a_2 = \frac{(m R_l + c L + \theta^2 R_l L + k C_p R_l L)}{R_l L}, \\ & a_3 = \frac{(c C_p R_l L + m L)}{R_l L}, a_4 = m C_p. \quad (72) \end{aligned}$$

Now using equation (52), the integral can be evaluated as

$$\begin{aligned}
\int_{-\infty}^{\infty} \frac{\omega^2}{\Delta_1(i\omega)\Delta_1^*(i\omega)} d\omega &= \frac{\pi}{a_4} \frac{\det \begin{bmatrix} b_3 & b_2 & b_1 & 0 \\ -a_4 & a_2 & -a_0 & 0 \\ 0 & -a_3 & a_1 & 0 \\ 0 & -a_4 & a_2 & a_0 \end{bmatrix}}{\det \begin{bmatrix} a_3 & -a_1 & 0 & 0 \\ -a_4 & a_2 & -a_0 & 0 \\ 0 & -a_3 & a_1 & 0 \\ 0 & -a_4 & a_2 & a_0 \end{bmatrix}} \\
&= \frac{\pi}{mC_p} \frac{\det \begin{bmatrix} 0 & 1 & 0 & 0 \\ -mC_p & \frac{mR_l + cL + \theta^2 R_l L + kC_p R_l L}{R_l L} & -\frac{k}{L} & 0 \\ 0 & -\frac{cC_p R_l L + mL}{R_l L} & \frac{cR_l + kL}{R_l L} & 0 \\ 0 & -mC_p & \frac{mR_l + cL + \theta^2 R_l L + kC_p R_l L}{R_l L} & \frac{k}{L} \end{bmatrix}}{\det \begin{bmatrix} \frac{cC_p R_l L + mL}{R_l L} & -\frac{cR_l + kL}{R_l L} & 0 & 0 \\ -mC_p & \frac{mR_l + cL + \theta^2 R_l L + kC_p R_l L}{R_l L} & -\frac{k}{L} & 0 \\ 0 & -\frac{cC_p R_l L + mL}{R_l L} & \frac{cR_l + kL}{R_l L} & 0 \\ 0 & -mC_p & \frac{mR_l + cL + \theta^2 R_l L + kC_p R_l L}{R_l L} & \frac{k}{L} \end{bmatrix}}. \tag{73}
\end{aligned}$$

Thus, from equation (71), we obtain the standard deviation of the voltage due to white-noise forcing as

5.2. Parameter optimisation

Like the previous case, m , c , and k are considered as fixed parameters. The aim is to find optimal parameter values, or

$$\sigma_v^2 = \frac{S_0 \pi (cR_l + kL) R_l^2 L}{c^2 C_p R_l^3 \theta^2 L + (c^3 C_p L + c C_p^2 k^2 L^2 - 2mC_p c k L + c C_p \theta^2 L^2 k + m\theta^2 L c + m^2 c) R_l^2 + (c^2 C_p L^2 k + mc^2 L + m\theta^2 L^2 k) R_l + mcL^2 k}. \tag{74}$$

The standard deviation of the derivative of the voltage $\dot{v}(t)$ can be obtained using equation (48) as

$$\begin{aligned}
\sigma_{\dot{v}}^2 &= \int_{-\infty}^{\infty} \omega^2 |H(\omega)|^2 \Phi_{x_b, x_b}(\omega) d\omega \\
&= S_0 \theta^2 \int_{-\infty}^{\infty} \frac{\omega^6}{\Delta_2(i\omega)\Delta_2^*(i\omega)} d\omega. \tag{75}
\end{aligned}$$

This can be evaluated as for the previous case with

$$n = 4, b_3 = 1, b_2 = 0, b_1 = 0, b_0 = 0 \tag{76}$$

with the same a_i , for $i = 0, \dots, 3$. Forming the \mathbf{N}_4 and \mathbf{D}_4 matrices in equation (52) and taking the ratio of the determinants of these matrices we have

parametric relationships, for the resistance (R_l), electro-mechanical coupling (θ), capacitance (C_p) and inductance (L). Using the expressions of σ_v and $\sigma_{\dot{v}}$ from equations (74) and (77), the zero crossing rate given by (33) can be calculated as

$$\begin{aligned}
N^+(0) = N^-(0) &= \frac{1}{2\pi} \frac{\sigma_{\dot{v}}}{\sigma_v} = \frac{1}{2\pi} \\
&\times \sqrt{\frac{(\theta^2 L c + mc) R_l^2 + (\theta^2 L^2 k + c^2 L + k^2 C_p L^2) R_l + c L^2 k}{m C_p R_l (c R_l + k L) L}}. \tag{78}
\end{aligned}$$

Using this expression, the rate of zero crossing of the voltage can be obtained directly from the harvester parameters.

$$\sigma_{\dot{v}}^2 = \frac{S_0 \pi ((\theta^2 L c + mc) R_l^2 + (\theta^2 L^2 k + c^2 L + k^2 C_p L^2) R_l + c L^2 k) R_l}{[c^2 C_p R_l^3 \theta^2 L + (c^3 C_p L + c C_p^2 k^2 L^2 - 2mC_p c k L + c C_p \theta^2 L^2 k + m\theta^2 L c + m^2 c) R_l^2 + (c^2 C_p L^2 k + mc^2 L + m\theta^2 L^2 k) R_l + mcL^2 k] m C_p}. \tag{77}$$

Parameter values can also be selected to set a desired zero crossing rate.

Using the expressions of σ_v in equation (74), together with the expression of v_c in terms of desired power P_c in equation (21), the expected rate of crossing can be obtained from equation (32). We aim to find parameter relationships such that the rate of crossing of power level P_c is maximised. Differentiating the resulting expression from equation (32) with respect to the resistance R_l and assuming no damping as before, after some algebra we obtain an optimal value of the resistance as

$$R_{l\text{opt}} = \sqrt{\frac{L^2 k (-\pi S_0 + m P_c \theta^2 + m P_c k C_p)}{C_p^3 L^2 P_c k^3 + (-2 m P_c k^2 L + 2 L^2 P_c \theta^2 k^2) C_p^2 + (-2 m P_c k L \theta^2 + \pi S_0 k L + m^2 P_c k + L^2 P_c \theta^4 k) C_p - \pi S_0 m + m^2 P_c \theta^2}} \quad (79)$$

Maximising the crossing rate in (32) with respect to the inductance L (assuming $c = 0$ again) we have the optimal value as

$$L_{\text{opt}} = \frac{2m(\pi S_0 - m P_c(\theta^2 + k C_p))}{k C_p(\pi S_0 - 2m P_c(\theta^2 + k C_p))}. \quad (80)$$

Notice that this optimum inductance does not depend on the load resistance, and hence this optimum inductance may be used in equation (79) to optimise both the resistance and inductance.

Next we aim to maximise the average fractional occupation time of the voltage $v(t)$ above the level v_c given in equation (42) by minimising $\frac{v_c^2}{2\sigma_v^2}$ as before. Assuming $c = 0$ again and differentiating the resulting expression with respect to R_l we obtain

$$R_{l\text{opt}} = \sqrt{\frac{m k L^2}{m^2 + C_p L^2 k (\theta^2 + k C_p) - 2 m C_p k L}}. \quad (81)$$

This expression matches with the results obtained in [24] for maximum power. The above expression is only exact for the undamped case. For the general case when $c \neq 0$, the optimisation process can be carried out numerically. In that case, the optimal value would differ from equation (81). The effect of damping is further investigated numerically in the next section.

Differentiating $\frac{v_c^2}{2\sigma_v^2}$ with respect to the inductance L , we obtain

$$(2 k^2 m C_p + R_l c C_p^2 k^2) L^2 - 2 k L m^2 - m^2 R_l c = 0. \quad (82)$$

The optimal value of L is obtained from the only positive solution of this equation as

$$L_{\text{opt}} = \frac{m}{k C_p}. \quad (83)$$

Again, notice that this optimum inductance does not depend on the load resistance.

6. Numerical verification

The expression derived for the number of voltage level crossings and the fractional occupational time will now be verified using a numerical example. As part of this verification the statistics of the voltage for the particular system will also be simulated. The mechanical part of the example will be fixed, and is based on the experimentally verified harvester of [57]. The baseline electrical circuit properties, namely the capacitance of the piezoelectric patch and the electro-mechanical coupling, are also taken from this paper. Only the

case without an inductor is considered here. The baseline values of the mechanical and electrical parameters are considered as

$$m = 9.12 \text{ g} \quad c = 0.218 \text{ Ns m}^{-1} \quad k = 4.10 \text{ kN m}^{-1}, \quad (84)$$

$$\theta = -4.57 \text{ mN V}^{-1} \quad C_p = 43.0 \text{ pF}. \quad (85)$$

Thus the natural frequency of the mechanical system (open circuit) is $\omega_n = 106.7$ Hz. The optimum load resistance from equation (69) without an inductor is $32.8 \text{ k}\Omega$, which will be used to determine suitable ranges of load resistance to simulate. For the value of the damping coefficient c given in equation (84), the damping ratio is $\zeta = 1.78\%$. In the numerical calculations we consider two additional values of the damping factor, namely $\zeta = 0.178\%$ and $\zeta = 17.8\%$. These two cases correspond to 10 times less and 10 times more damping compared to the baseline model in equation (84).

Suppose we apply broadband white noise force excitation with amplitude 0.01 N , so that $\Phi_{f_b, f_b} = 10^{-4} \text{ N}^2$, with a bandwidth of 600 Hz . The choice of the bandwidth of the excitation is a trade off and depends on the rate at which the response quantities of interest decay with frequency. Of course the analytical results have been derived for an infinite bandwidth, and hence the accuracy of the numerical results will be reduced by a finite bandwidth. For practical considerations, the smallest bandwidth possible is preferred, since a large excitation bandwidth requires a small time increment and thus an increase in the simulation time. The total simulation time should be long to ensure that the frequency increment in the spectra is small, which will ensure the accuracy of the response statistics calculated by integration in the frequency domain. Various difficulties in the simulation of random signals are discussed in the appendix, and in particular the relationship between time and frequency domains for simulated systems excited by random forces, compared to the ideal random responses assumed in the analysis.

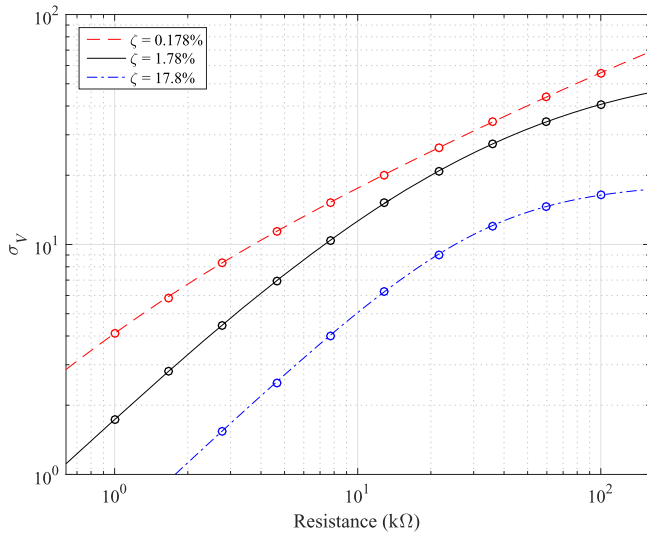


Figure 7. The standard deviation of the voltage as a function of load resistance. The lines are the analytical expressions (equation (60)) and the circles are the numerical simulations. The results for three different damping factors are shown.

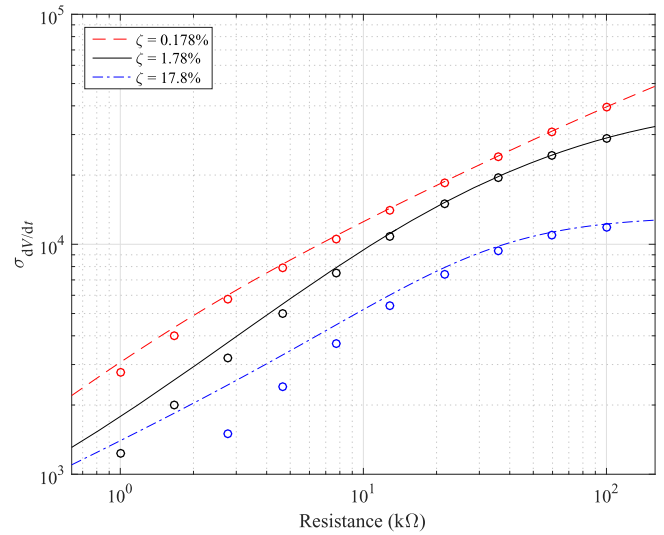


Figure 9. The standard deviation of the derivative of voltage as a function of load resistance for three different damping factors. The lines are the analytical expressions (equation (63)) and the circles are the numerical simulations. The results for three different damping factors are shown.

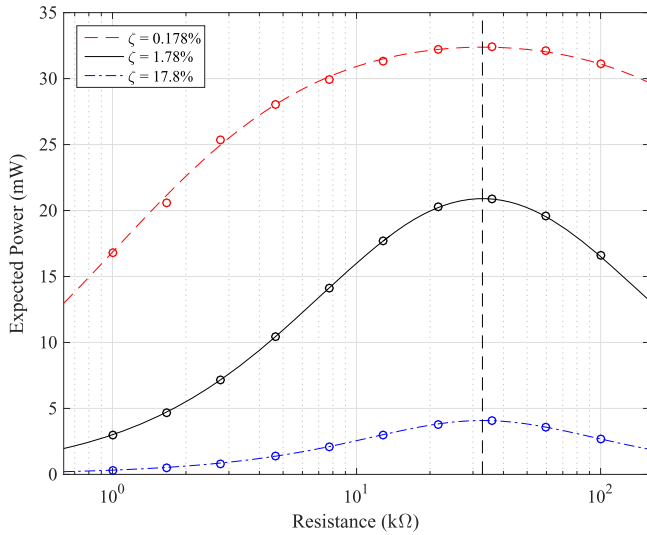


Figure 8. The expected power as a function of load resistance. The results for three different damping factors are shown. The lines are the analytical expressions and the circles are the numerical simulations. The vertical dashed line is the optimum resistance predicted for zero damping.

Figure 7 verifies the analytical expressions for the standard deviation of the voltage, where the response is simulated for 17.5 s. The expected power is shown in figure 8 and confirms that the maximum power occurs at approximately 33 kΩ. Lower damping values lead to higher standard deviation of the voltage and consequently higher expected power. A high value of the damping has the opposite effect. The accuracy of the analytical expressions is however independent of the damping values.

The standard deviation of the derivative of the voltage is shown in figure 9; clearly the accuracy of the numerical predications reduces for small values of load resistance. The reason is that the spectra of the derivative of voltage decreases

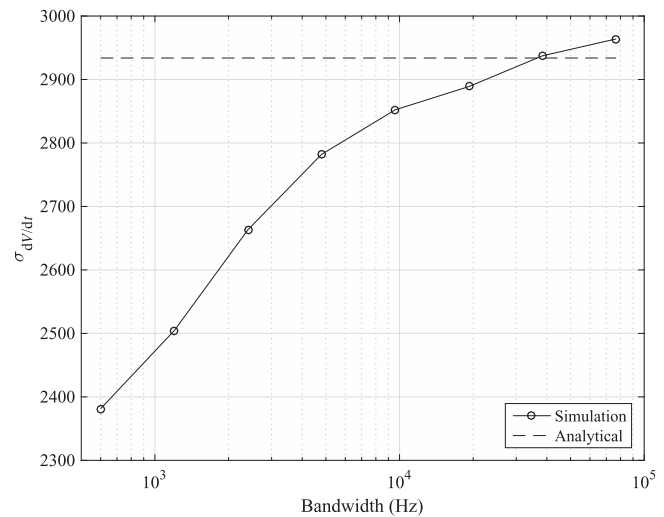


Figure 10. The standard deviation of the derivative of voltage as a function of excitation bandwidth for $R_l = 2$ kΩ and $\zeta = 1.78\%$. The dashed line is the analytical expression.

as $1/\omega$, although the leading coefficient in the denominator is small for low resistance values. Since the analytical expressions were obtained for perfect white noise excitation (i.e. infinite bandwidth) this gives errors in the predicted standard deviation of the derivative of voltage. To demonstrate this clearly we can increase the bandwidth of the force and calculate the standard deviation, while keeping the simulation time (and hence the frequency resolution of the spectra) constant. The results are shown in figure 10 for a load resistance of 2 kΩ and a damping ratio of 1.78%. Initially the simulated results converge towards the analytical result, but the character of the convergence changes at a bandwidth of 38.4 kHz. This change is due to spectrum of the derivative of

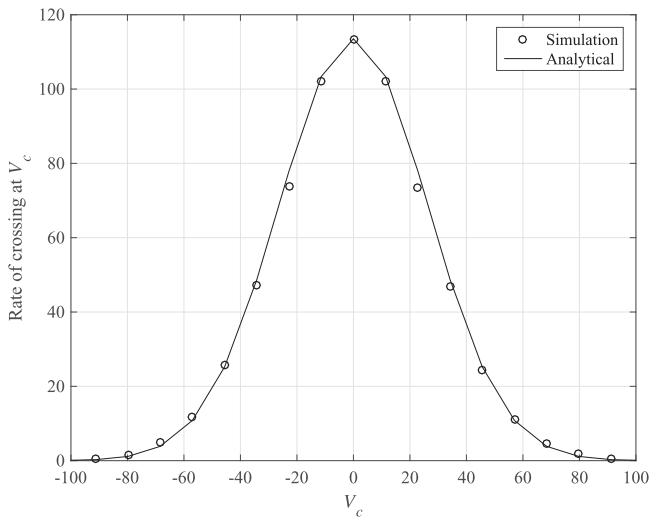


Figure 11. The rate that the voltage crosses the value V_c . The circles are the direct calculations from the voltage time series and the solid line are the estimates from the variance of V and \dot{V} given by equation (32).

voltage reaching the noise floor of the simulation due to the large number of sample points and the limited precision in the calculations due to the interpolation of the force. Additionally, the accuracy reduces significantly for high damping values in figure 9, because the higher damping ratio requires a higher bandwidth to capture the energy in the response. A damping factor of 17.8% is unusually high for a practical vibration energy harvester; this value is used simply to test the limit of accuracy of the analytical expressions derived in this paper.

Now consider the statistics of the voltage level crossings and the fractional occupational time. The load resistance is fixed at the optimum from equation (69) of 32.8 k Ω , which the simulations have shown to give the maximum power and an accurate estimate of voltage statistics with an excitation bandwidth of 600 Hz. The voltage time signal is renormalised using equation (A.5) to ensure the variance in the time domain is identical to that predicted in the frequency domain. Figure 11 shows the rate that the voltage crosses the value V_c and figure 12 shows the percentage of the voltage above V_c . In both cases the quantities are calculated from the computed response $V(t)$ and also by the analytical expressions derived in the paper. The figures clearly verify the accuracy of the analytical expressions.

7. Conclusions

Piezoelectric vibration energy harvesting under broadband random excitation is considered. A cantilever beam with PZT layers and a tip mass subjected to a base excitation is studied. Two cases, namely the harvesting circuit with and without an inductor, have been considered. The electromechanical model for both the cases are in general expressed by coupled second-order differential equations. When the base excitation to the system is considered to be a Gaussian random process, the

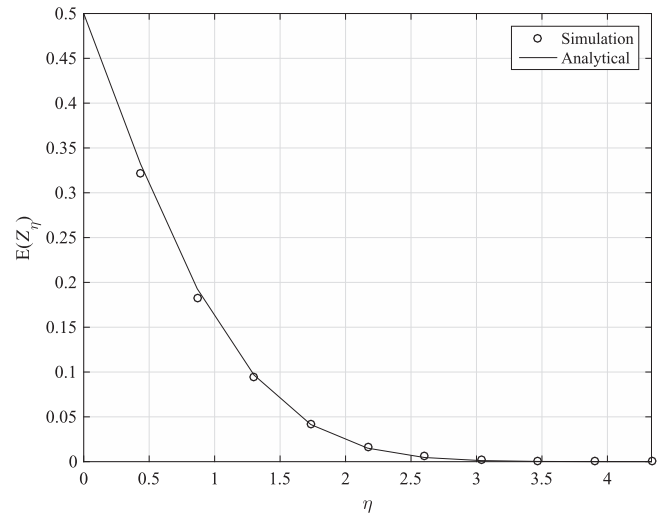


Figure 12. The percentage of the voltage above the value V_c . The circles are the direct calculation from the voltage time series and the solid line are the estimates from the variance of V and \dot{V} given by equation (43). $\eta = V_c/\sigma_V$.

output quantities such as displacement, velocity and voltage also become a Gaussian random process as the system is linear. Unlike conventional analysis and design where mainly the mean of the harvested power is considered, here we propose to utilise extreme values of the voltage response. This paper focuses on three key characteristics of the voltage response, namely (a) the number of level crossing, (b) the statistics of the response peaks above a certain level, and (c) the fractional occupational time. Exact closed-form analytical expressions describing these three characteristics have been derived for the voltage output for the two cases of energy harvesting circuits. This has been achieved by the amalgamation of linear random vibration theory and the electromechanical system models. Assuming the mass, damping and stiffness of the harvester as fixed parameters, optimal values of the resistance, electromechanical coupling, capacitance and inductance (where applicable) are obtained in closed-form. These optimal parameters maximise (a) the crossing rate of the voltage above a critical level and, (b) the fractional occupational time above a critical level, which in turn would maximise the harvested power.

The analytical results are validated using direct numerical simulation of the underlying time-series describing the input random excitation. Excellent agreement between the closed-form analytical results and simulation results have been observed for all three characteristics of the voltage response. Standard deviations of the voltage and its time-derivative play a crucial role in the derivation of the response characteristics. Analytical expressions describing these standard deviations match very well with simulation results for different values of the resistance.

This paper gives the basic mathematical framework for the design of vibration energy harvesters incorporating extreme response statistics. Future work should consider direct practical applications of the analytical expressions. Potential benefits arising from the design of vibration energy

harvesters with extreme response considerations should be explored further with suitable case studies.

Acknowledgments

SA gratefully acknowledges the support of Royal Society of London for the award of Wolfson Research Merit Award. GL gratefully acknowledges the support of the Polish National Science Center under Grant No. 2012/05/B/ST8/00080.

Appendix. Simulation of random signals

The verification of the analytical expressions requires the simulation of an energy harvester excited by a white noise excitation force. This section gives further details on the approach adopted for the simulation of random input signals. The excitation is assumed to have zero mean, and hence the response (both displacement and voltage) will also be zero mean. The variance of the voltage (for example) is then just the expected value of V^2 . We can calculate this expected value in the time domain or the frequency domain, since

$$E[V^2] = \int_{-\infty}^{\infty} S_{VV} d\omega = \int_{-\infty}^{\infty} |H(\omega)|^2 S_{ff} d\omega, \quad (\text{A.1})$$

where S_{VV} and S_{ff} are the spectral density of the voltage and force respectively and $H(\omega)$ is the frequency response function of the voltage.

There are a number of practical difficulties associated with calculating the variance, since our simulations require a finite simulation time and sample rate. A pure white noise excitation is not practical since the excitation at high frequencies requires a very short time increment. However the force is filtered by the resonance of the mechanical system and the voltage decays as $1/\omega^2$. Clearly from the calculation of variance in the frequency domain the contribution of high frequencies to the calculation of the variance of the voltage is small. Hence we can simulate a band-limited force. Note that the situation for the variance of \dot{V} is more difficult because \dot{V} only decays as $1/\omega$; this requires a large bandwidth for a given accuracy in the variance estimate. In fact the situation is worse for low load resistance, because the cubic term in the denominator of $H(\omega)$ is very small, which means that the frequency where the decay in $H(\omega)$ starts to behave as $1/\omega$ is much higher. Hence the bandwidth required is much higher.

The random force is simulated as an initial step, rather than at each iteration of the time integration. Time integration, such as the Runge–Kutta fourth order method used here, requires that the force is interrogated a number of times during each iteration. If each of these evaluations were completely random then the force would be inconsistent in time. The approach adopted here is to generate a band-limited force signal at a number of time samples and then interpolate intermediate values as necessary. The interpolation means that the sample rate must be significantly higher than force bandwidth, and a ratio of 100 is used in the simulations here.

Note that the interpolation does introduce errors in the simulation that resembles high frequency noise.

The other issue is linked to how the random force is simulated, which is related to the maximum simulated time, which determines the frequency increment in the FFT. One approach to generate the force is to low pass filter a random signal; however the low pass filters will not give a perfect spectrum, both because of the filter characteristics, and the random nature of the initial signal generation. The alternative used here is to recognise that the simulation time determines the periodicity of the simulated signal. Hence a Fourier series may be used, where the amplitude of each frequency component is constant for white noise but the phase is random. The force is given by

$$f(t) = \sum_{k=0}^n \sqrt{S_{ff}} \cos(k\Delta\omega t + \phi_k), \quad (\text{A.2})$$

where ϕ_k is the random phase and $\Delta\omega = 2\pi/T$ is the frequency resolution, where T is the simulation time. This gives a band limited flat spectrum in the frequency domain, where $n\Delta\omega$ is the bandwidth. This approach will give a good estimate of the response in the frequency domain, but will give a poor estimate of the statistics in the time domain.

There is an important distinction between the time and frequency domains, particularly for perfect white noise signals. Ideal noise signals have infinite length and hence are not periodic and the transformation from the time to frequency domain requires the Fourier transform. In contrast, the signals used for the simulation are periodic, which leads to an inconsistency because the Fourier transform of a periodic signal is not defined. However a relationship between the statistics in the time and frequency domains may be derived. Consider the statistics of the force, where the mean force is assumed to be zero. In the time domain the variance is

$$\begin{aligned} \sigma_{f,t}^2 &= \sum_{k=0}^n E[S_{ff} \cos^2(k\Delta\omega t + \phi_k)] \\ &= \sum_{k=0}^n S_{ff} E\left[\frac{1}{2} + \frac{1}{2} \cos(2k\Delta\omega t + 2\phi_k)\right] = \frac{nS_{ff}}{2}. \end{aligned} \quad (\text{A.3})$$

However in the frequency domain

$$\sigma_{f,\omega}^2 = \int_{-\infty}^{\infty} S_{ff} d\omega = \int_{-n\Delta\omega}^{n\Delta\omega} S_{ff} d\omega = 2nS_{ff} \Delta\omega. \quad (\text{A.4})$$

Hence, eliminating S_{ff} ,

$$\sigma_{f,\omega}^2 = 4\Delta\omega \sigma_{f,t}^2 = \frac{8\pi}{T} \sigma_{f,t}^2. \quad (\text{A.5})$$

The constant $\frac{8\pi}{T}$ is accurately reflected in the simulations, both for the force and the response. Typically the simulations will calculate the statistics in the frequency domain, whereas the analytical expressions effectively use the statistics in the time domain; equation (A.5) allows these two approaches to be compared.

References

- [1] Kim M, Dugundji J and Wardle B L 2015 Effect of electrode configurations on piezoelectric vibration energy harvesting performance *Smart Mater. Struct.* **24** 045026
- [2] Li P, Gao S and Cai H 2015 Modeling and analysis of hybrid piezoelectric and electromagnetic energy harvesting from random vibrations *Microsyst. Technol.* **21** 401–14
- [3] Karimi M, Tikani R, Ziaei-Rad S and Mirdamadi H 2015 Experimental and theoretical studies on piezoelectric energy harvesting from low-frequency ambient random vibrations *Proc. Inst. Mech. Eng. C* **25** 1496
- [4] Wu Y, Zuo L, Zhou W, Liang C and McCabe M 2014 Multi-source energy harvester for wildlife tracking *Proc. SPIE* **9057** 905704
- [5] Anton S R and Sodano H A 2007 A review of power harvesting using piezoelectric materials (2003–2006) *Smart Mater. Struct.* **16** R1
- [6] Erturk A and Inman D J 2009 An experimentally validated bimorph cantilever model for piezoelectric energy harvesting from base excitations *Smart Mater. Struct.* **18** 025009
- [7] Yang Y, Wu H and Soh C K 2015 Experiment and modeling of a two-dimensional piezoelectric energy harvester *Smart Mater. Struct.* **24** 125011
- [8] Aureli M, Prince C, Porfiri M and Peterson S D 2010 Energy harvesting from base excitation of ionic polymer metal composites in fluid environments *Smart Mater. Struct.* **19** 015003
- [9] Cellini F, Cha Y and Porfiri M 2013 Energy harvesting from fluid-induced buckling of ionic polymer metal composites *J. Intell. Mater. Syst. Struct.*
- [10] Wang L and Yuan F 2008 Vibration energy harvesting by magnetostrictive material *Smart Mater. Struct.* **17** 045009
- [11] Karaman I, Basaran B, Karaca H, Karsilayan A and Chumlyakov Y 2007 Energy harvesting using martensite variant reorientation mechanism in a NiMnGa magnetic shape memory alloy *Appl. Phys. Lett.* **90** 172505
- [12] Kim M, Dugundji J and Wardle B L 2015 Efficiency of piezoelectric mechanical vibration energy harvesting *Smart Mater. Struct.* **24** 055006
- [13] Beeby S P, Tudor M J and White N 2006 Energy harvesting vibration sources for microsystems applications *Meas. Sci. Technol.* **17** R175
- [14] Cook-Chennault K, Thambi N and Sastry A 2008 Powering MEMS portable devices: a review of non-regenerative and regenerative power supply systems with special emphasis on piezoelectric energy harvesting systems *Smart Mater. Struct.* **17** 043001
- [15] Karami M A and Inman D J 2012 Powering pacemakers from heartbeat vibrations using linear and nonlinear energy harvesters *Appl. Phys. Lett.* **100** 042901
- [16] Jang S, Jo H, Cho S, Mechtov K, Rice J, Sim S H, Jung H J, Yun C B, Spencer B Jr and Agha G 2010 Structural health monitoring of a cable-stayed bridge using smart sensor technology: deployment and evaluation *Smart Struct. Syst.* **6** 439–59
- [17] Park G, Rosing T, Todd M D, Farrar C R and Hodgkiss W 2008 Energy harvesting for structural health monitoring sensor networks *J. Infrastruct. Syst.* **14** 64–79
- [18] Shu Y C and Lien I C 2006 Analysis of power output for piezoelectric energy harvesting systems *Smart Mater. Struct.* **15** 1499–512
- [19] Liang J R and Liao W H 2012 Impedance modeling and analysis for piezoelectric energy harvesting systems *IEEE/ASME Trans. Mechatronics* **17** 1145–57
- [20] Kim H S, Kim J H and Kim J 2011 A review of piezoelectric energy harvesting based on vibration *Int. J. Precis. Eng. Manuf.* **12** 1129–41
- [21] Erturk A and Inman D J 2011 *Piezoelectric Energy Harvesting: Modelling and Application* (Sussex, UK: Wiley-Blackwell)
- [22] Lefeuve E, Badel A, Richard C and Guyomar D 2007 Energy harvesting using piezoelectric materials: case of random vibrations *J. Electroceramics* **19** 349–55 *Piezoceramics for End Users II Conf. (Hafjell, Norway, 05–08 March 2006)*
- [23] Halvorsen E 2008 Energy harvesters driven by broadband random vibrations *J. Microelectromech. Syst.* **17** 1061–71
- [24] Adhikari S, Friswell M I and Inman D J 2009 Piezoelectric energy harvesting from broadband random vibrations *Smart Mater. Struct.* **18** 115005
- [25] Litak G, Friswell M I and Adhikari S 2010 Magnetopiezoelectric energy harvesting driven by random excitations *Appl. Phys. Lett.* **96** 214103
- [26] Abdelkefi A, Nayfeh A H, Hajj M R and Najaf F 2012 Energy harvesting from a multifrequency response of a tuned bending-torsion system *Smart Mater. Struct.* **21** 075029
- [27] Borowiec B, Litak G, Friswell M I and Adhikari S 2014 Energy harvesting in a nonlinear cantilever piezoelectric beam system excited by random vertical vibrations *Int. J. Struct. Stab. Dyn.* **14** 1440018
- [28] Daqaq M F 2012 On intentional introduction of stiffness nonlinearities for energy harvesting under white Gaussian excitations *Nonlinear Dyn.* **69** 1063–79
- [29] Huang B, Hsieh C Y, Golnaraghi F and Moallem M 2015 Development and optimization of an energy-regenerative suspension system under stochastic road excitation *J. Sound Vib.* **357** 16–34
- [30] Ali S F, Adhikari S, Friswell M I and Narayanan S 2011 The analysis of piezomagnetoelastic energy harvesters under broadband random excitations *J. Appl. Phys.* **109** 074904
- [31] Jiang W A and Chen L Q 2013 Energy harvesting of monostable Duffing oscillator under Gaussian white noise excitation *Mech. Res. Commun.* **53** 85–91
- [32] Litak G, Borowiec B, Friswell M I and Adhikari S 2011 Energy harvesting in a magnetopiezoelectric system driven by random excitations with uniform and Gaussian distributions *J. Theor. Appl. Mech.* **49** 757–64
- [33] Jiang W A and Chen L Q 2014 An equivalent linearization technique for nonlinear piezoelectric energy harvesters under Gaussian white noise *Commun. Nonlinear Sci. Numer. Simul.* **19** 2897–904
- [34] Kim M, Dugundji J and Wardle B L 2015 Efficiency of piezoelectric mechanical vibration energy harvesting *Smart Mater. Struct.* **24** 055006
- [35] Lallart M, Wu Y C, Richard C, Guyomar D and Halvorsen E 2012 Broadband modeling of a nonlinear technique for energy harvesting *Smart Mater. Struct.* **21** 115006
- [36] Leadenham S and Erturk A 2015 Nonlinear M-shaped broadband piezoelectric energy harvester for very low base accelerations: primary and secondary resonances *Smart Mater. Struct.* **24** 055021
- [37] Li P, Gao S and Cai H 2015 Modeling and analysis of hybrid piezoelectric and electromagnetic energy harvesting from random vibrations *Microsyst. Technol.* **21** 401–14
- [38] Meimukhin D, Cohen N and Bucher I 2013 On the advantage of a bistable energy harvesting oscillator under band-limited stochastic excitation *J. Intell. Mater. Syst. Struct.* **24** 1736–46
- [39] Podder P, Mallick D and Roy S 2014 Bandwidth widening in nonlinear electromagnetic vibrational generator by combined effect of bistability and stretching *2014 14th Int. Conf. on Micro- and Nano-Technology for Power Generation and Energy Conversion Applications (PowerMEMS) (Hyogo, JAPAN Tsutomu Nakauchi Fdn, 18–21 November 2014) (Journal of Physics Conference Series vol 557) (Hyogo Int Assoc, IOP) pp 1742–6588*

- [40] Vandewater L A and Moss S D 2013 Probability-of-existence of vibro-impact regimes in a nonlinear vibration energy harvester *Smart Mater. Struct.* **22** 5
- [41] Wu Y C, Halvorsen E, Lallart M, Richard C and Guyomar D 2015 Stochastic modeling in the frequency domain for energy harvester with switching electronic interface *IEEE/ASME Trans. Mechatronics* **20** 50–60
- [42] Friswell M I, Bilgen O, Ali S F, Litak G and Adhikari S 2015 The effect of noise on the response of a vertical cantilever beam energy harvester (ZAMM) *Z. Angew. Math. Mech.* **95** 433–43
- [43] Yoon H and Youn B D 2014 Stochastic quantification of the electric power generated by a piezoelectric energy harvester using a time-frequency analysis under non-stationary random vibrations *Smart Mater. Struct.* **23** 045035
- [44] Zhao S and Erturk A 2013 Electroelastic modeling and experimental validations of piezoelectric energy harvesting from broadband random vibrations of cantilevered bimorphs *Smart Mater. Struct.* **22** 015002
- [45] Borowiec B, Litak G, Friswell M I, Ali S F, Adhikari S, Lees A W and Bilgen O 2013 Energy harvesting in piezoelectric systems driven by random excitations *Int. J. Struct. Stab. Dyn.* **14** 1340006
- [46] Zhao S and Erturk A 2013 On the stochastic excitation of monostable and bistable electroelastic power generators: relative advantages and tradeoffs in a physical system *Appl. Phys. Lett.* **102** 103902
- [47] Zhao S and Erturk A 2014 Deterministic and band-limited stochastic energy harvesting from uniaxial excitation of a multilayer piezoelectric stack *Sensors Actuators A* **214** 58–65
- [48] Vanmarcke E H 1983 *Random Fields* (Cambridge, MA: MIT Press)
- [49] Erturk A and Inman D J 2009 An experimentally validated bimorph cantilever model for piezoelectric energy harvesting from base excitations *Smart Mater. Struct.* **18** 025009
- [50] Erturk A and Inman D J 2008 A distributed parameter electromechanical model for cantilevered piezoelectric energy harvesters *Trans. ASME. J. Vib. Acoust.* **130** 041002
- [51] Erturk A and Inman D J 2008 On mechanical modeling of cantilevered piezoelectric vibration energy harvesters *J. Intell. Mater. Syst. Struct.* **19** 1311–25
- [52] Erturk A and Inman D J 2008 Issues in mathematical modeling of piezoelectric energy harvesters *Smart Mater. Struct.* **17** 065016
- [53] Lallart M, Wu Y C, Richard C, Guyomar D and Halvorsen E 2012 Broadband modeling of a nonlinear technique for energy harvesting *Smart Mater. Struct.* **21** 115006
- [54] Guyomar D, Badel A, Lefeuvre E and Richard C 2005 Toward energy harvesting using active materials and conversion improvement by nonlinear processing *IEEE Trans. Ultrason. Ferroelectr. Freq. Control* **52** 584–95
- [55] Wu Y C, Halvorsen E, Lallart M, Richard C and Guyomar D 2015 Stochastic modeling in the frequency domain for energy harvester with switching electronic interface *IEEE/ASME Trans. Mechatronics* **20** 50–60
- [56] D’hulst Y R, Sterken T, Puers R, Deconinck G and Driesen J 2010 Power processing circuits for piezoelectric vibration-based energy harvesters *IEEE/ASME Trans. Ind. Electron.* **57** 4170–7
- [57] duToit N E and Wardle B L 2007 Experimental verification of models for microfabricated piezoelectric vibration energy harvesters *AIAA J.* **45** 1126–37
- [58] Renno J M, Daqaq M F and Inman D J 2009 On the optimal energy harvesting from a vibration source *J. Sound Vib.* **320** 386–405
- [59] Lin Y K 1967 *Probabilistic Theory of Structural Dynamics* (New York: McGraw-Hill)
- [60] Nigam N C 1983 *Introduction to Random Vibration* (Cambridge, MA: MIT Press)
- [61] Bolotin V V 1984 *Random Vibration of Elastic Systems* (Hague: Martinus and Nijhoff Publishers)
- [62] Roberts J B and Spanos P D 1990 *Random Vibration and Statistical Linearization* (Chichester, England: Wiley)
- [63] Newland D E 1989 *Mechanical Vibration Analysis and Computation* (New York: Longman, Harlow and Wiley)
- [64] Papoulis A and Pillai S U 2002 *Probability, Random Variables and Stochastic Processes* 4th edn (Boston, USA: McGraw-Hill)
- [65] Abramowitz M and Stegun I A 1965 *Handbook of Mathematical Functions, with Formulas, Graphs, and Mathematical Tables* (New York, USA: Dover)